PROCEEDINGS OF SCIENCE

Inclusive quarkonium decay and production: from NRQCD to pNRQCD

Antonio Vairo[a,*]

[a] *Physics Department, TUM School of Natural Sciences, Technical University of Munich, James-Franck-Straße 1, 85748 Garching b. München, Germany*

E-mail: antonio.vairo@tum.de

This short account summarizes some of the progress made on heavy quarkonium inclusive decay and production in the framework of the pNRQCD factorization, which may be seen as a natural evolution of the NRQCD factorization established about 30 years ago.

Dedicated to the memory of Tom Mehen

The XVIth Quark Confinement and the Hadron Spectrum Conference (QCHSC24)
19-24 August, 2024
Cairns Convention Centre, Cairns, Queensland, Australia

*Speaker

 ISSN 1824-8039 . Published by SISSA Medialab.

PoS(QCHSC24)019

1. NRQCD

Rather surprisingly the first established effective field theory (EFT) for nonrelativistic fields involved two heavy particles rather than just one. This EFT is nonrelativistic quantum electrodynamics (NRQED) and its obvious extension to nonrelativistic quantum chromodynamics (NRQCD) [1]. Notoriously, however, in the first publication, QCD is mentioned (almost) only in the title. Applications of NRQCD were mostly restricted in the following years to lattice NRQCD [2, 3]. Few years after NRQCD, also the EFT for systems made of one heavy quark was formulated: the heavy quark effective theory (HQET) [4–7]. Differently from the somewhat slow start of NRQCD, HQET was an immediate breakthrough that revolutionized heavy flavor physics. The power counting of HQET allowed for a straightforward implementation of dimensional regularization, opening immediately the door to higher order perturbative calculations. For NRQCD, the real breakthrough came with its application to quarkonium annihilation and production [8, 9]. On the computational side, the understanding of how dimensional regularization works in NRQCD [10] allowed higher order precision calculations also for quarkonium. For some observables (e.g. near threshold $t\bar{t}$ observables or bottomonium ground state observables), the precision one can reach in weakly coupled NRQCD has no equivalent in HQET.

The phenomenological relevance of [9] can hardly be understated, as it put for the first time quarkonium annihilation on the solid ground of QCD and gave to the computation of quarkonium production observables a consistent and systematically improvable theoretical framework. Moreover, the NRQCD factorization is highly predictive and can be tested against numerous experimental findings.

At the basis of NRQCD is that *(i)* quarkonium is a nonrelativistic bound state, whose constituents, the heavy quarks/antiquarks of mass m_Q, have relative velocity $v \ll 1$; *(ii)* a quarkonium state, $|Q\rangle$, is mostly made by a heavy quark Q and antiquark $\bar{Q}$ pair in a color singlet configuration, but it also contains components, suppressed in v, where the heavy quark-antiquark pair is in a color octet component bound, for instance, with gluons; *(iii)* because of that quarkonium annihilation and production is described in NRQCD by matrix elements of four-fermion operators, $\mathcal{O}(N)$ in the case of annihilation and $\mathcal{O}^Q(N)$ in the case of production, projecting on both color singlet and color octet states identified by the generic quantum number N. The NRQCD factorization formula for the inclusive quarkonium width due to annihilation into light hadrons (l.h.) reads

$$\Gamma(Q \to \text{l.h.}) = 2 \sum_N \frac{\text{Im}\, f^{(N)}}{m_Q^{d_N-4}} \langle Q|\mathcal{O}(N)|Q\rangle, \tag{1}$$

where d_N is the dimension of the four-fermion operator. The factorization formula in NRQCD for the inclusive quarkonium production cross section reads

$$\sigma_{Q+X} = \sum_N \sigma_{Q\bar{Q}(N)} \langle \Omega|\mathcal{O}^Q(N)|\Omega\rangle, \tag{2}$$

where $|\Omega\rangle$ is the vacuum state. High energy modes are encoded in the short distance coefficients $f^{(N)}$ and $\sigma_{Q\bar{Q}(N)}$, while low energy contributions are in the long distance matrix elements (LDMEs) $\langle Q|\mathcal{O}(N)|Q\rangle$ and $\langle \Omega|\mathcal{O}^Q(N)|\Omega\rangle$, encoding contributions due to the scales $m_Q v$, $m_Q v^2$ and Λ_{QCD}.

Particularly simple is the case of P-wave quarkonium annihilation and hadroproduction, whose widths and cross sections, respectively, depend at leading order only on two LDMEs: a singlet one, labeled "1", and an octet one, labeled "8":

$$\Gamma(\chi_{QJ}(nP) \to \text{l.h.}) = 2\frac{\text{Im}\, f_1(^3P_J)}{m_Q^4}\, \langle \chi_{QJ}(nP)|O_1(^3P_J)|\chi_{QJ}(nP)\rangle + 2\frac{\text{Im}\, f_8(^3S_1)}{m_Q^2}\, \langle \chi_{QJ}(nP)|O_8(^1S_0)|\chi_{QJ}(nP)\rangle, \tag{3}$$

and

$$\sigma_{\chi_{QJ}(nP)+X} = \sigma_{Q\bar{Q}(^3P_J^{[1]})}\langle\Omega|O^{\chi_{QJ}}(^3P_J^{[1]})|\Omega\rangle + \sigma_{Q\bar{Q}(^3S_1^{[8]})}\langle\Omega|O^{\chi_{QJ}}(^3S_1^{[8]})|\Omega\rangle; \tag{4}$$

J is the angular momentum quantum number. The singlet matrix element may be expressed in terms of the quarkonium wavefunction at the origin, while the octet matrix element is an independent parameter to be fixed on data. According to the power counting of NRQCD, both the octet and the singlet LDMEs contribute to the same order. The octet matrix element is crucial to cancel infrared divergences present in the singlet short distance coefficients $\text{Im}\, f_1(^3P_J)$ and to make the above expressions finite, scale and scheme independent.

Some open issues remain in NRQCD. *(i)* The power counting of the EFT is not unique, as it still depends on the nonrelativistic scales $m_Q v$ and $m_Q v^2$. *(ii)* The bound state dynamics in the form of the Schrödinger equation is no yet apparent, as soft fields, those scaling with $m_Q v$, are still dynamical. *(iii)* While color singlet LDMEs may be related to the quarkonium wavefunction at the origin, although the corresponding Schrödinger equation is not defined in NRQCD, color octet LDMEs are free parameters, depending on the quarkonium state, that need to be fitted on data. As an example, for P-wave bottomonium and charmonium states below threshold, decay widths and cross sections, besides the three wavefunctions, depend on three octet matrix elements for the decay widths and three independent ones for the cross sections.

2. Quarkonium annihilation in pNRQCD

The open issues of NRQCD are solved by potential NRQCD, pNRQCD, the EFT that follows from NRQCD by integrating out modes of soft momentum and energy [11–13]. Suitable for the description of charmonium and excited bottomonium inclusive decay and production is the version of pNRQCD that applies to strongly coupled bound states [12, 14–22].

We start from the spectral decomposition of the NRQCD Hamiltonian, H_{NRQCD}, in the $Q\bar{Q}$ sector of the Hilbert space,

$$H_{\text{NRQCD}}\big|_{Q\bar{Q}} = \sum_n \int d^3x_1\, d^3x_2\, |\underline{\text{n}};\boldsymbol{x}_1,\boldsymbol{x}_2\rangle\, E_n(\boldsymbol{x}_1,\boldsymbol{x}_2;\boldsymbol{\nabla}_1,\boldsymbol{\nabla}_2)\, \langle\underline{\text{n}};\boldsymbol{x}_1,\boldsymbol{x}_2|, \tag{5}$$

where $|\underline{\text{n}};\boldsymbol{x}_1,\boldsymbol{x}_2\rangle$ are orthonormal states made of a heavy quark, a heavy antiquark, and some light degrees of freedom labeled by n. E_n are operators in the coordinate, momentum and spin of the $Q\bar{Q}$. In the static limit, $E_n = E_n^{(0)}$ are the different energy excitations of a static $Q\bar{Q}$ pair. They

may be computed in lattice QCD as a function of the $Q\bar{Q}$ distance. The eigenstates of the NRQCD Hamiltonian in the $Q\bar{Q}$ sector can be written as

$$|Q(n,\boldsymbol{P})\rangle = \int d^3x_1 d^3x_2\, \phi_{Q(n,\boldsymbol{P})}(\boldsymbol{x}_1,\boldsymbol{x}_2)\, |\underline{\mathrm{n}};\boldsymbol{x}_1,\boldsymbol{x}_2\rangle, \tag{6}$$

where $\boldsymbol{P}$ is the quarkonium center of mass momentum and n is the set of quantum numbers that identifies the quarkonium state. The functions $\phi_{Q(n,\boldsymbol{P})}(\boldsymbol{x}_1,\boldsymbol{x}_2)$ are eigenfunctions of $E_n(\boldsymbol{x}_1,\boldsymbol{x}_2;\boldsymbol{\nabla}_1,\boldsymbol{\nabla}_2)$. The quarkonium state $|Q(\boldsymbol{P})\rangle$ corresponds to the state $|Q(0,\boldsymbol{P})\rangle$, and the quarkonium state at rest, $|Q\rangle$, corresponds to $|Q(0,\boldsymbol{0})\rangle$.

In strongly coupled pNRQCD, the non interacting part of the Hamiltonian is given by

$$H_{\mathrm{pNRQCD}} = \int d^3x_1\, d^3x_2\; S_n^\dagger\, h_n(\boldsymbol{x}_1,\boldsymbol{x}_2;\boldsymbol{\nabla}_1,\boldsymbol{\nabla}_2)\, S_n, \tag{7}$$

where S_n is a color singlet field containing a $Q\bar{Q}$. The operator h_n is obtained by matching the NRQCD energy E_n; it may be identified with the quantum mechanical Hamiltonian entering the Schrödinger equation of the bound state. The matching can be performed order by order in $1/m_Q$ by expanding the NRQCD Hamiltonian and the states $|\underline{\mathrm{n}};\boldsymbol{x}_1,\boldsymbol{x}_2\rangle$ using quantum mechanical perturbation theory. The Hamiltonian at leading order in the velocity expansion has the form

$$h_n(\boldsymbol{x}_1,\boldsymbol{x}_2;\boldsymbol{\nabla}_1,\boldsymbol{\nabla}_2) = -\frac{\boldsymbol{\nabla}_1^2}{2m_Q} - \frac{\boldsymbol{\nabla}_2^2}{2m_Q} + V^{(0;n)}(\boldsymbol{x}_1,\boldsymbol{x}_2). \tag{8}$$

The matching fixes the static potential $V^{(0;n)}$ to be the static energy $E_n^{(0)}$. As a consequence of the matching, the functions $\phi_{Q(n,\boldsymbol{P})}$ are eigenfunctions of the pNRQCD Hamiltonian h_n.

The pNRQCD factorization formula for the quarkonium annihilation matrix elements reads

$$\begin{aligned}\langle Q|O(N)|Q\rangle = \frac{1}{\langle \boldsymbol{P}=\boldsymbol{0}|\boldsymbol{P}=\boldsymbol{0}\rangle} \int d^3x_1 d^3x_2 d^3x_1' d^3x_2'\, \phi_Q(\boldsymbol{x}_1-\boldsymbol{x}_2) \\ \Big[-V_{O(N)}(\boldsymbol{x}_1,\boldsymbol{x}_2;\boldsymbol{\nabla}_1,\boldsymbol{\nabla}_2)\delta^{(3)}(\boldsymbol{x}_1-\boldsymbol{x}_1')\delta^{(3)}(\boldsymbol{x}_2-\boldsymbol{x}_2')\Big]\, \phi_Q^*(\boldsymbol{x}_1'-\boldsymbol{x}_2'),\end{aligned} \tag{9}$$

where ϕ_Q is the quarkonium wavefunction at rest in pNRQCD (corresponding to the state $n=0$ and $\boldsymbol{P}=\boldsymbol{0}$); $\langle \boldsymbol{P}=\boldsymbol{0}|\boldsymbol{P}=\boldsymbol{0}\rangle = \int d^3R$ is a normalization factor. The operator $V_{O(N)}$ is determined by matching NRQCD with pNRQCD order by order in $1/m_Q$ via quantum mechanical perturbation theory.

On the example of the matching of the P-wave annihilation matrix elements entering the leading order expression of the width, we get [16, 17]

$$\langle \chi_{QJ}(nP)|O_1(^3P_J)|\chi_{QJ}(nP)\rangle = \frac{3N_c}{2\pi}|R'_{nP}(0)|^2, \tag{10}$$

$$\langle \chi_{QJ}(nP)|O_8(^1S_0)|\chi_{QJ}(nP)\rangle = \frac{1}{9N_c m_Q^2}\,\frac{3N_c}{2\pi}|R'_{nP}(0)|^2\mathcal{E}_3, \tag{11}$$

where $N_c=3$ is the number of colors, R_{nP} is the radial part of the wavefunction, R'_{nP} its derivative and

$$\mathcal{E}_3 = \frac{1}{2N_c}\int_0^\infty dt\, t^3 \langle \Omega|gE^{i,a}(t,\boldsymbol{0})\Phi_{ab}(t,0)gE^{i,b}(0,\boldsymbol{0})|\Omega\rangle \tag{12}$$

is a universal chromoelectric correlator, ideally to be computed in lattice QCD. The quantity $\Phi_{ab}(t,0)$ is a Wilson line in the adjoint representation connecting $(t,\mathbf{0})$ with $(0,\mathbf{0})$. The correlator is universal in the sense that it does not depend on the quarkonium state. The P-wave annihilation widths in pNRQCD at leading order in the velocity expansion then read

$$\Gamma(\chi_{QJ}(nP)\to \text{l.h.}) = \frac{3N_c}{\pi m_Q^4}\left|R'_{nP}(0)\right|^2\left[\text{Im}\, f_1(^3P_J) + \frac{\text{Im}\, f_8(^3S_1)}{9N_c}\,\mathcal{E}_3\right]. \tag{13}$$

We note that the quarkonium state dependence factorizes, the infrared divergence affecting $\text{Im}\, f_1(^3P_J)$ cancels against the chromoelectric correlator $\mathcal{E}_3$ that depends on a renormalization scale Λ, and the P-wave decay widths of bottomonium and charmonium states below threshold depend now on only 4 nonperturbative parameters: three wavefunctions and one universal correlator [16, 17].

The universal correlator $\mathcal{E}_3(\Lambda)$ can be obtained from a fit to the ratios of decay rates $\Gamma(\chi_{c0}(1P)\to \text{l.h.})/\Gamma(\chi_{c1}(1P)\to \text{l.h.})$, $\Gamma(\chi_{c1}(1P)\to \text{l.h.})/\Gamma(\chi_{c2}(1P)\to \text{l.h.})$, $\Gamma(\chi_{c0}(1P)\to \text{l.h.})/\,\Gamma(\chi_{c0}(1P)\to\gamma\gamma)$, and $\Gamma(\chi_{c2}(1P)\to \text{l.h.})/\Gamma(\chi_{c2}(1P)\to\gamma\gamma)$ at leading order in v. The electromagnetic decays depend on the wavefunctions only. In the $\overline{\text{MS}}$ scheme, we obtain [18]

$$\mathcal{E}_3(1\text{ GeV}) = 2.05^{+0.94}_{-0.65}. \tag{14}$$

$\mathcal{E}_3(\Lambda)$ at different scales follows from the one loop renormalization group improved expression ($\beta_0 = 11N_c/3 - 2n_f/3$ with n_f the number of light flavors)

$$\mathcal{E}_3(\Lambda) = \mathcal{E}_3(\Lambda') + \frac{12(N_c^2-1)}{N_c\beta_0}\log\frac{\alpha_s(\Lambda')}{\alpha_s(\Lambda)}, \tag{15}$$

where $\alpha_s = g^2/(4\pi)$ is the strong coupling. Computing the wavefunction with several potential models, we get for the charmonium P-wave annihilation widths [18]

$$\Gamma(\chi_{c0}(1P)\to \text{l.h.}) = 8.3^{+3.0}_{-3.1}\text{ MeV}, \tag{16}$$
$$\Gamma(\chi_{c1}(1P)\to \text{l.h.}) = 0.42^{+0.06\,+0.28}_{-0.06-0.22}\text{ MeV}, \tag{17}$$
$$\Gamma(\chi_{c2}(1P)\to \text{l.h.}) = 1.4^{+0.6}_{-0.6}\text{ MeV}, \tag{18}$$

to be compared with the PDG values 10.6 ± 0.6 MeV, 0.552 ± 0.041 MeV and 1.60 ± 0.09 MeV [23], respectively. For the bottomonium P-wave annihilation widths using the same universal correlator, we obtain [18]

$$\Gamma(\chi_{b0}(nP)\to \text{l.h.}) = 1.07^{+0.33}_{-0.37}\text{ MeV}, \tag{19}$$
$$\Gamma(\chi_{b1}(nP)\to \text{l.h.}) = 0.14\pm0.06\text{ MeV}, \tag{20}$$
$$\Gamma(\chi_{b2}(nP)\to \text{l.h.}) = 0.28^{+0.09}_{-0.10}\text{ MeV}, \tag{21}$$

which are predicted to be independent of the principal quantum number $n = 1,2,3$ at leading order in the velocity expansion. The results for bottomonium are proper predictions of pNRQCD, as they exploit the universality of the chromoelectric correlator.

Updated results for S- and P-wave quarkonium inclusive and electromagnetic widths in the context of pNRQCD factorization can be found in [18]. Older and in part superseded results are in [16, 17].

3. Quarkonium hadroproduction in pNRQCD

A similar factorization as the one that holds for the annihilation decay widths also holds for the inclusive production cross section of quarkonium. The relevant color singlet and color octet four-fermion operators for hadroproduction of quarkonia in NRQCD have the form

$$O^{Q}(N_{\text{color singlet}}) = \chi^\dagger \mathcal{K}_N \psi \mathcal{P}_{Q(\boldsymbol{P}=\boldsymbol{0})} \psi^\dagger \mathcal{K}'_N \chi, \tag{22}$$

$$O^{Q}(N_{\text{color octet}}) = \chi^\dagger \mathcal{K}_N T^a \psi \Phi_\ell^{\dagger ab}(0) \mathcal{P}_{Q(\boldsymbol{P}=\boldsymbol{0})} \Phi_\ell^{bc}(0) \psi^\dagger \mathcal{K}'_N T^c \chi, \tag{23}$$

where ψ and $\chi^\dagger$ are the fields that annihilate a heavy quark and antiquark respectively, and $\Phi_\ell^{ab}(x)$ is a Wilson line along the direction ℓ in the adjoint representation required to ensure the gauge invariance of the color octet LDME [24]. The operator $\mathcal{P}_{Q(\boldsymbol{P})}$ projects onto a state containing a heavy quarkonium Q with momentum $\boldsymbol{P}$. $\mathcal{P}_{Q(\boldsymbol{P})}$ commutes with the NRQCD Hamiltonian as the number of quarkonia is conserved and is diagonalized by the same eigenstates of the NRQCD Hamiltonian, therefore, it has the form

$$\mathcal{P}_{Q(\boldsymbol{P})} = \sum_{n\in\mathbb{S}} |Q(n,\boldsymbol{P})\rangle\langle Q(n,\boldsymbol{P})|. \tag{24}$$

The sum extends over $\mathbb{S}$, which are all states where the $Q\bar{Q}$ is in a color singlet at the origin in the static limit. This is a necessary condition to produce a quarkonium.

According to (6), the projector $\mathcal{P}_{Q(\boldsymbol{P})}$ depends on the wavefunction $\phi_{Q(n,\boldsymbol{P})}$ with $n \in \mathbb{S}$. At leading order $\phi_{Q(n,\boldsymbol{P})}$ is an eigenfunction of the pNRQCD Hamiltonian (8) with $V^{(0;n)}$ the energy of a static Wilson loop in the presence of disconnected gluon fields. Lattice QCD determinations of $V^{(0;n)}$ for $n \in \mathbb{S}$ and $n \neq 0$ are not available yet. One expects, however, that disconnected gluon fields produce mainly a constant shift to the potentials, e.g. in the form of a glueball mass. This is supported by the large N_c limit: the vacuum expectation value of a Wilson loop with additional disconnected gluon fields factorizes into the vacuum expectation value of the Wilson loop times the vacuum expectation value of the additional gluon fields up to corrections of order $1/N_c^2$. If the slopes of the static potentials are the same for all $n \in \mathbb{S}$, then we can approximate [19]

$$\phi_{Q(n,\boldsymbol{P})}(\boldsymbol{x}_1,\boldsymbol{x}_2) \approx e^{i\boldsymbol{P}\cdot(\boldsymbol{x}_1+\boldsymbol{x}_2)/2} \phi_Q^{(0)}(\boldsymbol{x}_1-\boldsymbol{x}_2), \tag{25}$$

where $\phi_Q^{(0)}$ is the leading order *quarkonium* wavefunction in the center of mass frame.

The pNRQCD factorization formula for the quarkonium production LDMEs at leading order reads

$$\begin{aligned}\langle\Omega|O^{Q}(N)|\Omega\rangle = \frac{1}{\langle \boldsymbol{P}=\boldsymbol{0}|\boldsymbol{P}=\boldsymbol{0}\rangle} \int d^3x_1 d^3x_2 d^3x'_1 d^3x'_2\, \phi_Q^{(0)}(\boldsymbol{x}_1-\boldsymbol{x}_2) \\ \times \left[-V_{O^Q(N)}(\boldsymbol{x}_1,\boldsymbol{x}_2;\boldsymbol{\nabla}_1,\boldsymbol{\nabla}_2)\delta^{(3)}(\boldsymbol{x}_1-\boldsymbol{x}'_1)\delta^{(3)}(\boldsymbol{x}_2-\boldsymbol{x}'_2)\right] \phi_Q^{(0)\,*}(\boldsymbol{x}'_1-\boldsymbol{x}'_2).\end{aligned} \tag{26}$$

The operator $V_{O^Q(N)}$ is determined by matching the NRQCD LDMEs to pNRQCD order by order in $1/m_Q$ via quantum mechanical perturbation theory, similarly to what done for the NRQCD matrix elements entering the annihilation widths.

On the example of the matching of the P-wave LDMEs entering at leading order the cross section $pp \to \chi_{QJ} + X$, see (4), we eventually get [19, 20]

$$\langle\Omega|\mathcal{O}^{\chi_{QJ}}({}^3P_J^{[1]})|\Omega\rangle = (2J+1)\frac{3N_c}{2\pi}|R'_{nP}(0)|^2, \tag{27}$$

$$\langle\Omega|\mathcal{O}^{\chi_{QJ}}({}^3S_1^{[8]})|\Omega\rangle = (2J+1)\frac{3N_c}{2\pi}|R'_{nP}(0)|^2\frac{1}{9N_c m_Q^2}\mathcal{E}_{11}, \tag{28}$$

where LDMEs are polarization summed. The dimensionless gluonic correlator, $\mathcal{E}_{11}$, appearing in the octet LDME is

$$\mathcal{E}_{11} = \frac{3}{N_c}\int_0^\infty dt\, t \int_0^\infty dt'\, t' \,\langle\Omega|\Phi_\ell^{\dagger ab}\Phi^{\dagger ad}(0;t)gE^{d,i}(t)gE^{e,i}(t')\Phi^{ec}(0;t')\Phi_\ell^{bc}|\Omega\rangle. \tag{29}$$

For a suitable choice of the sign of ℓ^0, the fields in $gE^{e,j}(t')\Phi^{ec}(0;t')\Phi_\ell^{bc}$ are time ordered ($\mathcal{T}$) and those in $\Phi_\ell^{\dagger ab}\Phi^{\dagger ad}(0;t)gE^{d,i}(t)$ are anti-time ordered ($\bar{\mathcal{T}}$). Hence the correlator $\mathcal{E}_{11}$ may be interpreted as the cut diagram shown in figure 1. The above expressions imply (at leading order in v) the universality of the ratios

$$\frac{m_Q^2\langle\Omega|\mathcal{O}^{\chi_{QJ}}({}^3S_1^{[8]})|\Omega\rangle}{\langle\Omega|\mathcal{O}^{\chi_{QJ}}({}^3P_J^{[1]})|\Omega\rangle} = \frac{\mathcal{E}_{11}}{9N_c}.$$

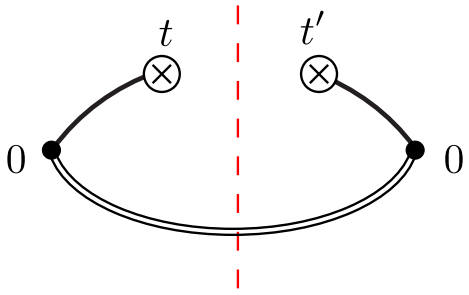

Figure 1: Representation of the chromoelectric fields and Wilson lines in (29) as a cut diagram: $\otimes$ stand for insertions of chromoelectric fields at the times t and t', filled circles for the spacetime origin, double lines for Schwinger lines, and solid lines for gauge-completion Wilson lines in the ℓ direction.

For the pNRQCD expressions of the LDMEs to be consistent with perturbative QCD, they must reproduce the same infrared divergences. At two loop accuracy and at the lowest order in the relative momentum q of the Q and $\bar{Q}$, the infrared divergences in the NRQCD LDMEs can be cast in the infrared factor

$$\sum_N \int_0^\infty d\lambda'\,\lambda'\langle\Omega|\bar{\mathcal{T}}\left\{\Phi_\ell^{\dagger c'b}\Phi_p^{\dagger a'c'}(\lambda')[p^\mu q^\nu F^{a'}_{\nu\mu}(\lambda' p)]\right\}|N\rangle$$
$$\times\int_0^\infty d\lambda\,\lambda\langle N|\mathcal{T}\left\{\Phi_\ell^{bc}[p^\mu q^\nu F^a_{\nu\mu}(\lambda p)]\Phi_p^{ac}(\lambda)\right\}|\Omega\rangle. \tag{30}$$

The sum over N contains all possible intermediate states, p is half the center-of-mass momentum of the $Q\bar{Q}$ pair, $F^a_{\nu\mu}$ is the QCD field strength tensor, and $\Phi_p^{ab}(\lambda)$ is an adjoint Wilson line along p

[24–26]. Since in the expression (30) a momentum q comes from each side of the cut, the infrared factor contributes to the production of a color-singlet P-wave state. In the rest frame of the $Q\bar{Q}$ pair: $\boldsymbol{p} = 0$, $q^0 = 0$, $\Phi_p^{ab}(\lambda) = \Phi^{ab}(0;t)$ with $t = \sqrt{p^2}\lambda$, $p^\mu q^\nu F^a_{\nu\mu}(\lambda p) = -\sqrt{p^2} q^i E^{a\,i}(t)$ and the expression (30) reduces to a term proportional to the contact term $V_{O^{\chi_{QJ}}({}^3S_1^{[8]})}$ in momentum space. Hence, the pNRQCD expressions for the color-octet1t LDMEs reproduce the same infrared divergences of the NRQCD infrared factor [20]. Furthermore, the one-loop running of $\mathcal{E}_{11}$,

$$\frac{d}{d\log\Lambda}\mathcal{E}_{11}(\Lambda) = 6\frac{N_c^2-1}{N_c}\frac{\alpha_s}{\pi}, \tag{31}$$

implies that $\frac{d}{d\log\Lambda}\langle O^{\chi_{QJ}}({}^3S_1^{[8]})\rangle = \frac{2(N_c^2-1))\alpha_s}{3N_c^2\pi m_Q^2}\langle O^{\chi_{QJ}}({}^3P_J^{[1]})\rangle$. This agrees with the one-loop evolution equation derived in perturbative NRQCD [9]. For a related study on the shape function formalism see [27].

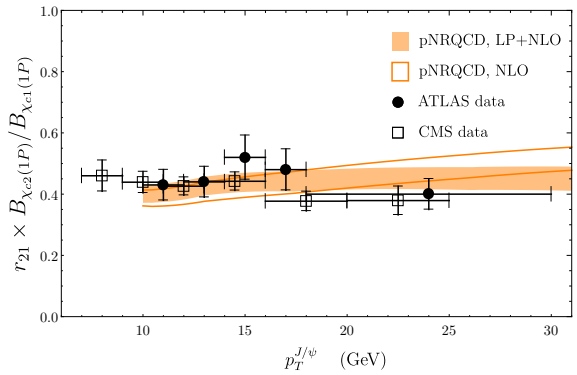

Figure 2: Ratio r_{21} of the $\chi_{c2}(1P)$ and $\chi_{c1}(1P)$ differential cross sections at the LHC center of mass energy $\sqrt{s} = 7$ TeV and in the rapidity range $|y| < 0.75$, with fitted $\mathcal{E}_{11}$, compared to ATLAS [28] and CMS [29] measurements, from [20].

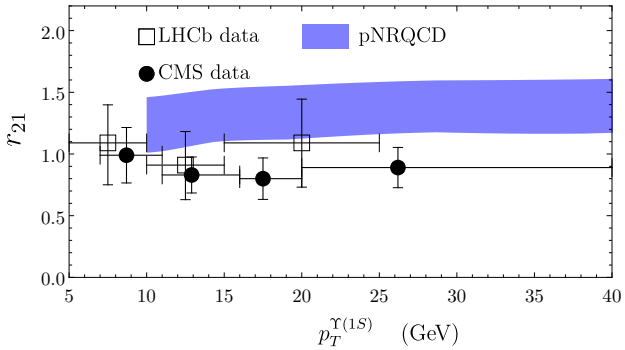

Figure 3: Ratio of the $\chi_{b2}(1P)$ and $\chi_{b1}(1P)$ differential cross sections at the LHC center of mass energy $\sqrt{s} = 7$ TeV and in the rapidity range $2 < y < 4.5$ compared with LHCb [30] and CMS [31] measurements, from [20].

The chromoelectric correlator $\mathcal{E}_{11}$ may be extracted by fitting the ratio,

$$r_{21} = \frac{d\sigma_{\chi_{c2}(1P)}/dp_T}{d\sigma_{\chi_{c1}(1P)}/dp_T}, \tag{32}$$

on ATLAS and CMS data, see figure 2. At leading order in the velocity expansion, the ratio does not depend on the wavefunction, but exclusively on $\mathcal{E}_{11}$. We obtain at the charm mass scale [20]

$$\mathcal{E}_{11}(\Lambda = 1.5\ \text{GeV}) = 2.8 \pm 1.7\,. \tag{33}$$

Like the correlator $\mathcal{E}_3$ entering the P-wave quarkonium annihilation width, also the correlator $\mathcal{E}_{11}$ relevant for P-wave quarkonium hadroproduction is universal: it does not depend neither on the flavor of the heavy quark nor on the quarkonium state. The universal nature of the correlator allows to use it to compute cross sections for quarkonia with different principal quantum numbers and for bottomonia (once accounted for the running) without having to fit new octet LDMEs. We can test the universality of the correlator, and the validity of the pNRQCD factorization for hadroproduction, by looking at the ratio $(d\sigma_{\chi_{b2}(1P)}/dp_T)/(d\sigma_{\chi_{b1}(1P)}/dp_T)$ that at leading order in pNRQCD depends only on $\mathcal{E}_{11}$ (at the scale of the bottom mass, according to the running given by (31)) and therefore is expected to be the same also for $2P$ and $3P$ bottomonium states. The result compared to LHCb and CMS data is shown in figure 3.

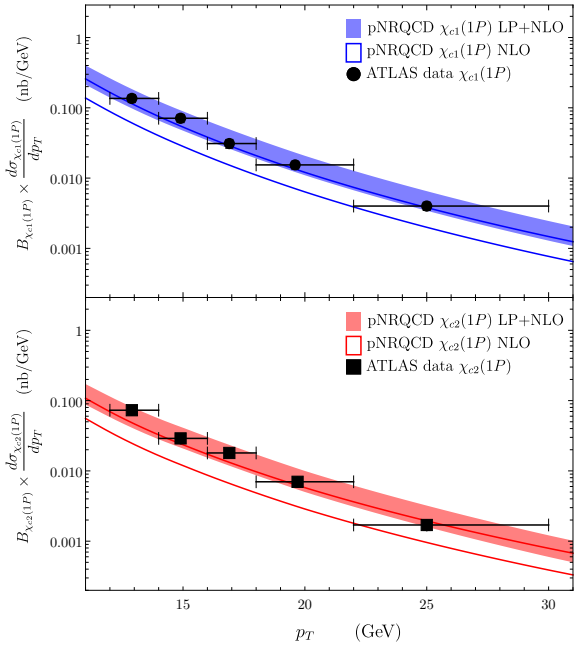

Figure 4: Production cross sections of $\chi_{c1}(1P)$ and $\chi_{c2}(1P)$ at the LHC center of mass energy $\sqrt{s} = 7$ TeV and in the rapidity range $|y| < 0.75$ compared with ATLAS measurements [28], from [20].

To evaluate the absolute values of the P-wave quarkonium hadroproduction cross sections from the pNRQCD factorization formulas (27) and (28) valid at leading order in the velocity expansion, we need the derivatives of the quarkonium wavefunctions at the origin. For charmonium, these can be extracted from the electromagnetic widths $\Gamma(\chi_{c0,2}(1P) \to \gamma\gamma)$, which satisfy at leading order

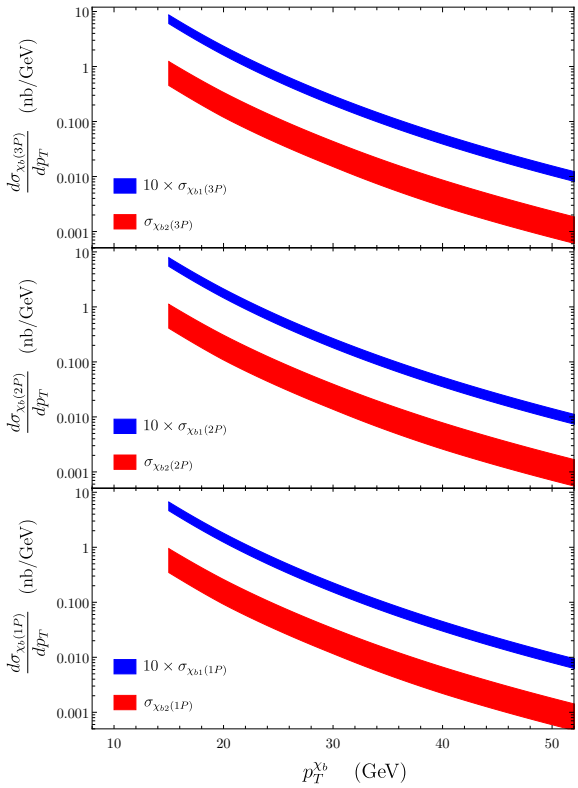

Figure 5: Production cross sections of $\chi_{b1}(nP)$ and $\chi_{b2}(nP)$ ($n = 1$, 2, and 3) at the LHC center of mass energy $\sqrt{s} = 7$ TeV in the rapidity range $2 < y < 4.5$, from [20].

a factorization formula like (13), but without octet contribution. The results are plotted in figure 4 and compared with ATLAS data. Because for P-wave bottomonium the electromagnetic widths are not known experimentally, we assign to the derivative of the $\chi_{bJ}(nP)$ wavefunctions at the origin values determined averaging several potential model predictions. The results are plotted in figure 5; these are real predictions as measurements are not available yet.

Further results on S- and P-wave quarkonium inclusive electromagnetic and hadroproduction in the context of pNRQCD factorization can be found in [18–22, 33]. From [22], in figure 6 we show the production cross sections for J/ψ and $\psi(2S)$, in figure 7 the production cross sections for $\Upsilon(2S)$ and $\Upsilon(3S)$, and in figure 8 the production cross section for $\Upsilon(1S)$ (with the caveat that $\Upsilon(1S)$ has been treated as a strongly coupled bound state). The LDMEs for $\Upsilon(1S)$, $\Upsilon(2S)$ and $\Upsilon(3S)$ are related through universality relations of the same type as those that relate the LDMEs for $\chi_{bJ}(1P)$, $\chi_{bJ}(2P)$ and $\chi_{bJ}(3P)$.

4. Conclusions

From an effective field theory point of view, potential NRQCD ideally completes the program started 30 years ago with the NRQCD factorization, as it further factorizes the lower nonrelativistic energy scales still dynamical in NRQCD. It supplies factorization formulas for quarkonium inclusive

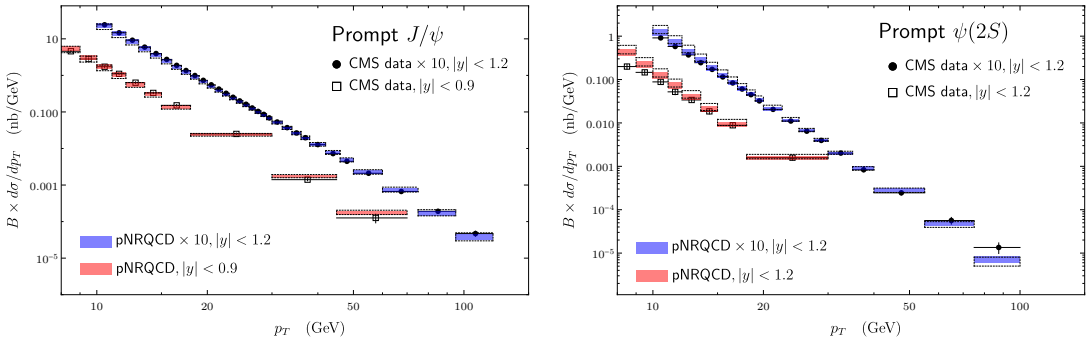

Figure 6: Production cross sections of prompt J/ψ and $\psi(2S)$ at the LHC center of mass energy $\sqrt{s} = 7$ TeV compared to CMS data [34, 35], B is the dimuon branching fraction, from [22].

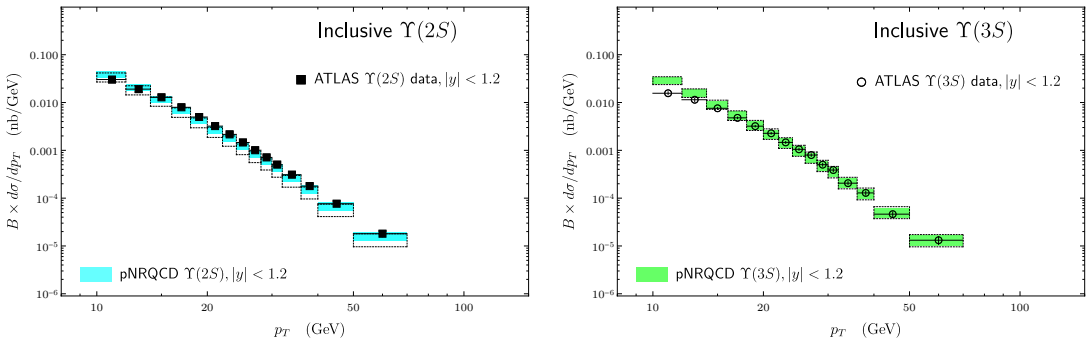

Figure 7: Production cross sections of inclusive $\Upsilon(2S)$ and $\Upsilon(3S)$ at the LHC center of mass energy $\sqrt{s} = 7$ TeV compared to ATLAS data [36], B is the dimuon branching fraction, from [22].

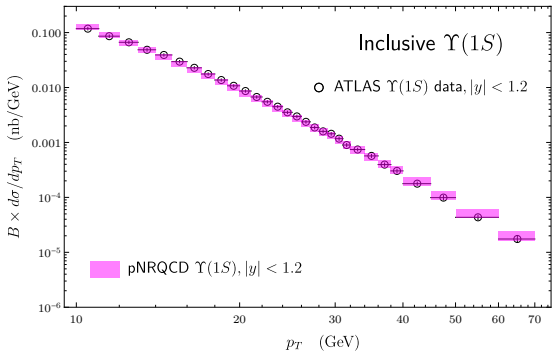

Figure 8: Production cross section of inclusive $\Upsilon(1S)$ at the LHC center of mass energy $\sqrt{s} = 7$ TeV compared to ATLAS data [36], B is the dimuon branching fraction, from [22].

annihilation widths and production cross sections that relate octet matrix elements with different principal quantum number and heavy flavor. Octet matrix elements are a major source of uncertainty in the NRQCD factorization. Reducing this source of uncertainty enhances significantly the predictive power of the theory.

In pNRQCD, the nonperturbative input for the decay and production observables is provided

by the quarkonium wavefunctions at the origin and some universal correlators. The wavefunctions at the origin, at least at leading order, may be extracted straightforwardly from the electromagnetic decays. For P-wave charmonia, data for these decays are available, but not for P-wave bottomonia, which is an important systematic limitation in the determination of the bottomonium observables. Beyond leading order, also electromagnetic decay widths depend on correlators and the extraction becomes much less straightforward [17, 18]. Wavefunctions could also be determined theoretically as eigenfunctions of the pNRQCD Hamiltonian with the potentials computed in lattice QCD. It is possible that in the near future, as the lattice determinations of these potentials improve (see e.g. [37]), this will become the most reliable way to determine the quarkonium wavefunctions. Concerning the correlators, they may be fitted on data as has been reviewed in these proceedings, but ideally should also be computed in lattice QCD. Studies in this direction are under way [38].

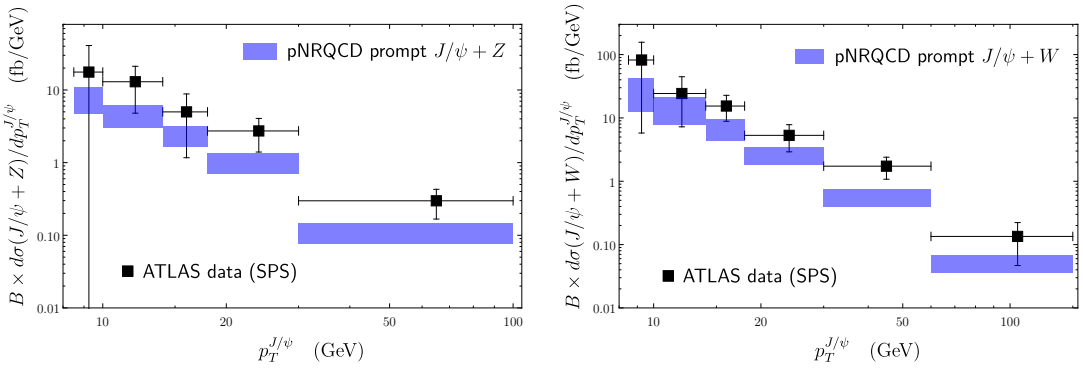

Figure 9: Production cross sections of prompt $J/\psi + Z$ (left) and prompt $J/\psi + W$ (right) at the LHC center of mass energy $\sqrt{s} = 8$ TeV for $|y^{J/\psi}| < 2.1$ in pNRQCD compared to ATLAS data [39, 40], B is the dimuon branching fraction, from [22].

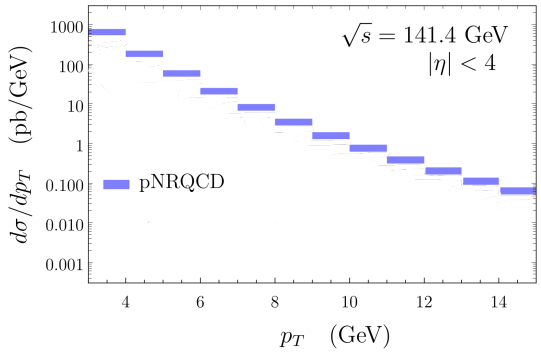

Figure 10: pNRQCD prediction for the p_T-differential cross sections for J/ψ from ep collisions at the EIC with center of mass energy $\sqrt{s} = 141.4$ GeV and pseudo-rapidity region $|\eta| < 4$, from [22].

Systematic improvements of the pNRQCD expressions for decay widths and cross sections come from higher order weak coupling corrections in the short distance coefficients and higher order corrections in the velocity expansion. Higher order corrections in the velocity expansion have different sources. They arise from higher dimensional operators in the NRQCD factorization

formula, from higher order corrections in the pNRQCD expansion of the NRQCD long distance matrix elements, and from higher order corrections to the wavefunctions originating from higher order corrections in the pNRQCD potential and quantum mechanical perturbation theory.

The pNRQCD factorization can be applied to several quarkonium production processes, like photoproduction [22], production associated with a weak gauge boson, see figure 9, production at the Electron-Ion Collider (EIC), see figure 10, and others. Extensions of the formalism to quarkonium production at heavy ion colliders and quarkonium exotica (hybrids, tetraquarks, ...) production in hadron colliders are also being studied.

Acknowledgements

After 20 years from our first discussion at an INT program in Seattle, I met with Tom Mehen for the last time at this conference. This conference paper is dedicated to his memory.

I thank Nora Brambilla, Hee Sok Chung, Daniel Müller and Xiang-Peng Wang for collaboration on the work presented in these proceedings.

References

[1] W. E. Caswell and G. P. Lepage, Phys. Lett. B **167** (1986), 437-442.

[2] B. A. Thacker and G. P. Lepage, Phys. Rev. D **43** (1991), 196-208.

[3] G. P. Lepage, L. Magnea, C. Nakhleh, U. Magnea and K. Hornbostel, Phys. Rev. D **46** (1992), 4052-4067 [arXiv:hep-lat/9205007 [hep-lat]].

[4] N. Isgur and M. B. Wise, Phys. Lett. B **232** (1989), 113-117.

[5] E. Eichten and B. R. Hill, Phys. Lett. B **234** (1990), 511-516.

[6] N. Isgur and M. B. Wise, Phys. Lett. B **237** (1990), 527-530.

[7] N. Isgur and M. B. Wise, Phys. Rev. Lett. **66** (1991), 1130-1133.

[8] G. T. Bodwin, E. Braaten and G. P. Lepage, Phys. Rev. D **46** (1992), R1914-R1918 [arXiv:hep-lat/9205006 [hep-lat]].

[9] G. T. Bodwin, E. Braaten and G. P. Lepage, Phys. Rev. D **51** (1995), 1125-1171 [erratum: Phys. Rev. D **55** (1997), 5853] [arXiv:hep-ph/9407339 [hep-ph]].

[10] A. V. Manohar, Phys. Rev. D **56** (1997), 230-237 [arXiv:hep-ph/9701294 [hep-ph]].

[11] A. Pineda and J. Soto, Nucl. Phys. B Proc. Suppl. **64** (1998), 428-432 [arXiv:hep-ph/9707481 [hep-ph]].

[12] N. Brambilla, A. Pineda, J. Soto and A. Vairo, Nucl. Phys. B **566** (2000), 275 [arXiv:hep-ph/9907240 [hep-ph]].

[13] N. Brambilla, A. Pineda, J. Soto and A. Vairo, Rev. Mod. Phys. **77** (2005), 1423 [arXiv:hep-ph/0410047 [hep-ph]].

[14] N. Brambilla, A. Pineda, J. Soto and A. Vairo, Phys. Rev. D **63** (2001), 014023 [arXiv:hep-ph/0002250 [hep-ph]].

[15] A. Pineda and A. Vairo, Phys. Rev. D **63** (2001), 054007 [erratum: Phys. Rev. D **64** (2001), 039902] [arXiv:hep-ph/0009145 [hep-ph]].

[16] N. Brambilla, D. Eiras, A. Pineda, J. Soto and A. Vairo, Phys. Rev. Lett. **88** (2002), 012003 [arXiv:hep-ph/0109130 [hep-ph]].

[17] N. Brambilla, D. Eiras, A. Pineda, J. Soto and A. Vairo, Phys. Rev. D **67** (2003), 034018 [arXiv:hep-ph/0208019 [hep-ph]].

[18] N. Brambilla, H. S. Chung, D. Müller and A. Vairo, JHEP **04** (2020), 095 [arXiv:2002.07462 [hep-ph]].

[19] N. Brambilla, H. S. Chung and A. Vairo, Phys. Rev. Lett. **126** (2021) no.8, 082003 [arXiv:2007.07613 [hep-ph]].

[20] N. Brambilla, H. S. Chung and A. Vairo, JHEP **09** (2021), 032 [arXiv:2106.09417 [hep-ph]].

[21] N. Brambilla, H. S. Chung, A. Vairo and X. P. Wang, Phys. Rev. D **105** (2022) no.11, L111503 [arXiv:2203.07778 [hep-ph]].

[22] N. Brambilla, H. S. Chung, A. Vairo and X. P. Wang, JHEP **03** (2023), 242 [arXiv:2210.17345 [hep-ph]].

[23] M. Tanabashi *et al.* [Particle Data Group], Phys. Rev. D **98** (2018) no.3, 030001.

[24] G. C. Nayak, J. W. Qiu and G. F. Sterman, Phys. Lett. B **613** (2005), 45-51 [arXiv:hep-ph/0501235 [hep-ph]].

[25] G. C. Nayak, J. W. Qiu and G. F. Sterman, Phys. Rev. D **72** (2005), 114012 [arXiv:hep-ph/0509021 [hep-ph]].

[26] G. C. Nayak, J. W. Qiu and G. F. Sterman, Phys. Rev. D **74** (2006), 074007 [arXiv:hep-ph/0608066 [hep-ph]].

[27] H. S. Chung, JHEP **07** (2023), 007 [arXiv:2303.17240 [hep-ph]].

[28] G. Aad *et al.* [ATLAS], JHEP **07** (2014), 154 [arXiv:1404.7035 [hep-ex]].

[29] S. Chatrchyan *et al.* [CMS], Eur. Phys. J. C **72** (2012), 2251 [arXiv:1210.0875 [hep-ex]].

[30] R. Aaij *et al.* [LHCb], JHEP **10** (2014), 088 [arXiv:1409.1408 [hep-ex]].

[31] V. Khachatryan *et al.* [CMS], Phys. Lett. B **743** (2015), 383-402 [arXiv:1409.5761 [hep-ex]].

[32] R. Aaij *et al.* [LHCb], Eur. Phys. J. C **74** (2014) no.10, 3092 [arXiv:1407.7734 [hep-ex]].

[33] N. Brambilla, M. Butenschoen and X. P. Wang, [arXiv:2411.16384 [hep-ph]].

[34] S. Chatrchyan *et al.* [CMS], JHEP **02** (2012), 011.

[35] V. Khachatryan *et al.* [CMS], Phys. Rev. Lett. **114** (2015) no.19, 191802 [arXiv:1502.04155 [hep-ex]].

[36] G. Aad *et al.* [ATLAS], Phys. Rev. D **87** (2013) no.5, 052004 [arXiv:1211.7255 [hep-ex]].

[37] M. Eichberg and M. Wagner, PoS **LATTICE2024** (2025), 117 [arXiv:2411.11640 [hep-lat]].

[38] N. Brambilla, S. Datta, M. Janer, V. Leino, J. Mayer-Steudte, P. Petreczky and A. Vairo, TUM-EFT 189/24.

[39] G. Aad *et al.* [ATLAS], Eur. Phys. J. C **75** (2015) no.5, 229 [arXiv:1412.6428 [hep-ex]].

[40] M. Aaboud *et al.* [ATLAS], JHEP **01** (2020), 095 [arXiv:1909.13626 [hep-ex]].